https://doi.org/10.20965/jrm.2006.p0076

Paper:

Feed Rate Control Using Fuzzy Reasoning for a Mold Polishing Robot

Fusaomi Nagata*, and Keigo Watanabe**

*Fukuoka Industrial Technology Center
3-6-1 Norimatsu, Yahatanishi, Kitakyushu, Fukuoka 807-0831, Japan
E-mail: nagata@fitc.pref.fukuoka.jp
**Graduate School of Science and Engineering, Saga University
1 Honjomachi, Saga 840-8502, Japan
E-mail: watanabe@me.saga-u.ac.jp
[Received July 15, 2005; accepted November 7, 2005]

Reducing time cost of polishing process is a major issue in metallic mold manufacturing. The feed rate, i.e., tangential velocity, of a polishing robot is generally limited to maintain stable contact with workpieces having a large curvature. We propose a feed rate generator using fuzzy reasoning for polishing robots that regulates the feed rate along free-formed surfaces appropriately. The smaller the curvature of the model designed by a 3D CAD, the larger the distance between two adjacent cutter location data (CL data) steps generated by the main processor of CAM. Therefore, given curvature results in acquiring the distance between two adjacent steps of CL data. We also propose a hybrid position/force controller with the feed rate generator enabling the robot to conduct polishing efficiently. Experiments show promising results.

Keywords: CAD/CAM, feed rate, fuzzy reasoning, hybrid position/force control, polishing robot

1. Introduction

Industrial robots have progressed dramatically in different industrial fields to where open-architecture industrial robots with kinematics and servo control are being developed. Using such robots, we can develop skillful applications without conventional complicated teaching. A 3-dimensional (3D) robot sander proposed for manufacturing attractively designed furniture [1, 2] realized nontaught operation concerning the position and orientation of the sanding tool attached to the robot arm. Other several polishing robots using force controllers have also been developed, enabling successful finishing in each manufacturing process [3–7].

In poly ethylene terephthalate (PET) bottle mold manufacturing, 3D CAD/CAM and NC machine tools are widely used. These advanced systems have dramatically streamlined metallic mold design and manufacture. The polishing process following NC machining, however, has yet to be automated due to the complex requirements of free-formed surfaces that must be addressed in mold polishing. No advanced polishing robots have, to our knowledge, been commercialized for metallic molds, due to poor polishing quality, long cycle time, and complex operation. This means ongoing dependence on skilled workers whose dexterous force and skillful trajectory control using abrasive tools prevent automation. To automate the polishing process, we are developing a mold polishing robot, focusing on reducing the cycle time of polishing process.

We propose a feed rate generator using fuzzy reasoning to shorten polishing time and design a hybrid position/force controller with weak coupling. Feed rate is the tangential velocity along a curved surface. To reduce total polishing time, the feed rate should be given as large as possible according to the curvature of each workpiece. A faster velocity is achievable within areas with smaller curvature. A slower velocity must, however, be given to suppress unstable behavior when the curvature is large. Robot operators thus pay due attention to systematically regulating during polishing, which is difficult. Our proposed feed rate generator, which uses fuzzy reasoning, gives appropriate feed rates based on the curvature. Experiments confirmed the effectiveness and potential of the proposed hybrid position/force controller using the feed rate generator installed in a mold polishing robot.

2. Curvature Along Desired Trajectory

A target workpiece with a curved surface is generally designed using 3D CAD/CAM, generating CL data via the main-processor of CAM. CL data, originally used for NC machine tools, consists of sequential cutting points along a zigzag or whirl path on the model surface. In this approach, desired trajectory $\boldsymbol{r}(k) \in \Re^{6\times 1}$ at discrete time k is generated along CL data calculated with a linear approximation along a curved surface. The i-th step is written by

$$\tilde{\boldsymbol{P}}(i) = [P_x(i)\ P_y(i)\ P_z(i)\ N_x(i)\ N_y(i)\ N_z(i)]^T \quad \ldots \quad (1)$$

$$\{N_x(i)\}^2 + \{N_y(i)\}^2 + \{N_z(i)\}^2 = 1 \quad \ldots \quad (2)$$

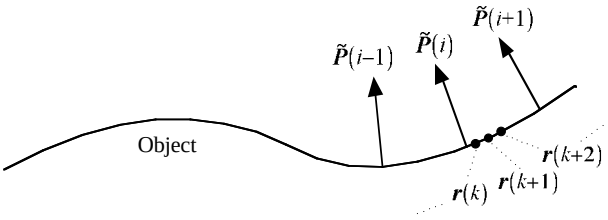

Fig. 1. Relationship between CL data $\tilde{\boldsymbol{P}}(i)$ and desired trajectory $\boldsymbol{r}(k)$.

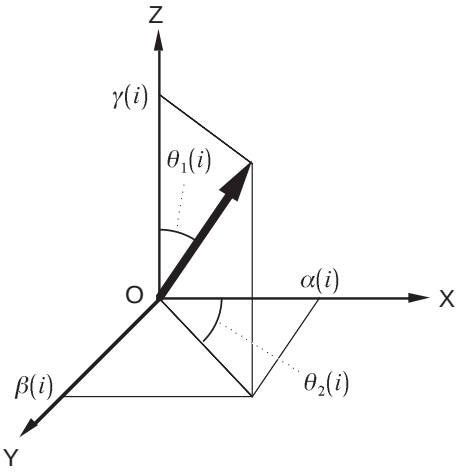

Fig. 2. Normalized tool vector $\boldsymbol{n}(i)$ represented by $\theta_1(i)$ and $\theta_2(i)$ in robot base coordinates.

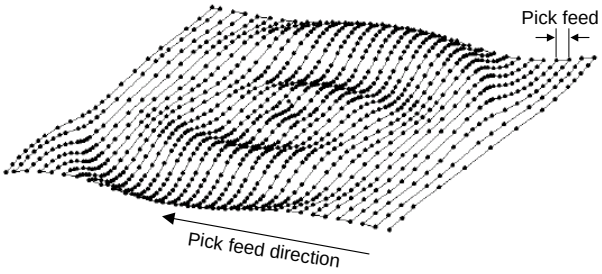

Fig. 3. Image of curvature and point density in CL data.

where $\boldsymbol{P}(i) = [P_x(i) \;\; P_y(i) \;\; P_z(i)]^T$ and $\boldsymbol{N}(i) = [N_x(i) \;\; N_y(i) \;\; N_z(i)]^T$ are the position vector and normalized orientation vector. $\boldsymbol{r}(k)$ is obtained by using linear equations and feed rate. $\boldsymbol{r}(k)$ is represented by

$$\boldsymbol{r}(k) = \left[\boldsymbol{x}_d^T(k) \;\; \boldsymbol{o}_d^T(k)\right]^T \quad \ldots\ldots\ldots \quad (3)$$

where $\boldsymbol{x}_d(k) = [x_{dx}(k) \;\; x_{dy}(k) \;\; x_{dz}(k)]^T$ and $\boldsymbol{o}_d(k) = [o_{d\alpha}(k) \;\; o_{d\beta}(k) \;\; o_{d\gamma}(k)]^T$ are the position and orientation components. $\boldsymbol{r}(k)$ is calculated using both CL data and feed rate $\boldsymbol{v}_t(k)$ represented by

$$\boldsymbol{v}_t(k) = \left[v_{tx}(k) \;\; v_{ty}(k) \;\; v_{tz}(k)\right]^T \quad \ldots\ldots\ldots \quad (4)$$

where $\|\boldsymbol{v}_t(k)\|$ is regulated by the feed rate generator in the next section and is constant during $\boldsymbol{r}(k) \in [\tilde{\boldsymbol{P}}(i), \tilde{\boldsymbol{P}}(i+1)]$. The relationship between CL data $\tilde{\boldsymbol{P}}(i)$ and desired trajectory $\boldsymbol{r}(k)$ is shown in **Fig.1**. Assuming $\boldsymbol{r}(k) \in [\tilde{\boldsymbol{P}}(i), \tilde{\boldsymbol{P}}(i+1)]$, we obtain $\boldsymbol{r}(k)$ as follows, first deriving a direction vector $\boldsymbol{t}(i)$ by

$$\boldsymbol{t}(i) = \boldsymbol{P}(i+1) - \boldsymbol{P}(i) \quad \ldots\ldots\ldots \quad (5)$$

so that each directional feed rate is obtained by

$$v_{tj}(k) = \left\|\boldsymbol{v}_t(k)\right\| \frac{t_j(i)}{\left\|\boldsymbol{t}(i)\right\|} \qquad (j = x,y,z). \quad \ldots \quad (6)$$

Using sampling width Δt, each component of the desired position $\boldsymbol{x}_d(k)$ is given by

$$x_{dj}(k) = x_{dj}(k-1) + v_{tj}(k)\Delta t \qquad (j = x,y,z). \quad (7)$$

Desired orientation $\boldsymbol{o}_d(k)$ is considered next. We define two angles $\theta_1(i), \theta_2(i)$ **(Fig.2)**. $\theta_1(i)$ and $\theta_2(i)$ are the tool angle of inclination and rotation. Using $\theta_1(i)$ and $\theta_2(i)$, each component of $\boldsymbol{n}(i)$ is represented by

$$\alpha(i) = \sin\theta_1(i)\cos\theta_2(i) \quad \ldots\ldots\ldots \quad (8)$$
$$\beta(i) = \sin\theta_1(i)\sin\theta_2(i) \quad \ldots\ldots\ldots \quad (9)$$
$$\gamma(i) = \cos\theta_1(i). \quad \ldots\ldots\ldots \quad (10)$$

Desired tool angles $\theta_{r1}(k)$, $\theta_{r2}(k)$ of inclination and rotation at discrete time k are calculated as

$$\theta_{rj}(k) = \theta_j(i) + \{\theta_j(i+1) - \theta_j(i)\} \frac{\left\|\boldsymbol{x}_d(k) - \boldsymbol{P}(i)\right\|}{\left\|\boldsymbol{t}(i)\right\|} \quad \ldots\ldots\ldots \quad (11)$$

where $j = 1,2$. If Eq.(11) is substituted into Eqs.(8)-(10), yielding

$$o_{d\alpha}(k) = \sin\theta_{r1}(k)\cos\theta_{r2}(k) \quad \ldots\ldots\ldots \quad (12)$$
$$o_{d\beta}(k) = \sin\theta_{r1}(k)\sin\theta_{r2}(k) \quad \ldots\ldots\ldots \quad (13)$$
$$o_{d\gamma}(k) = \cos\theta_{r1}(k). \quad \ldots\ldots\ldots \quad (14)$$

$\boldsymbol{x}_d(k)$ and $\boldsymbol{o}_d(k)$ are used for the desired position and desired force direction given to a workpiece.

The feed rate is the most important parameter for reducing total polishing time. The feed rate should be as large as possible, but if a workpiece has a large curvature or the cutter path has small edges caused by constant pick feed (**Fig.3**), then the stability of force control tends to worsen. The main-processor of CAM calculates cutter path $\boldsymbol{P}(i)$ with linear approximation so that the workpiece can be machined within the tolerance of a designed model. The larger the curvature, the higher its density. Accordingly, given curvature results in acquiring distance $d(i) = \|\boldsymbol{P}(i+1) - \boldsymbol{P}(i)\|$ between two adjacent steps of CL data and its increment $\Delta d(i) = d(i+1) - d(i)$. **Fig.3** shows curvature and point density in CL data. In the next section, we discuss a systematic feed rate control using fuzzy reasoning.

Table 1. Consequent constants for fuzzy reasoning. The upper table is tuned for $d(i)$ and the lower for $\Delta d(i)$. Note that $v_{base} = v_{\max} - v_{\min}$.

c_1^A	c_2^A	c_3^A	c_4^A	c_5^A	c_6^A
$v_{\min}+0.1v_{base}$	$v_{\min}+0.3v_{base}$	$v_{\min}+0.9v_{base}$	$v_{\min}+1.5v_{base}$	$v_{\min}+2.1v_{base}$	$v_{\min}+2.7v_{base}$
c_1^B	c_2^B	c_3^B	c_4^B	c_5^B	c_6^B
$-v_{\min}$	$-0.7v_{\min}$	$-0.3v_{\min}$	$0.3v_{\min}$	$0.7v_{\min}$	$v_{\min}$

3. Feed Rate Control Using Fuzzy Reasoning

We propose a fuzzy feed rate generator that produces suitable feed rates based on $d(i)$ and $\Delta d(i)$. The fuzzy feed rate generator consists of two simple fuzzy reasoning parts whose consequent parts are constant. When current position $\boldsymbol{x}(k) = [x(k)\ y(k)\ z(k)]^T$ of an abrasive tool at discrete time k is $\boldsymbol{x}(k) \in [\boldsymbol{P}(i), \boldsymbol{P}(i+1)]$, feed rate norm $v_{norm}(i)$ and its compensation $\Delta v_{norm}(i)$ are estimated by

Rule 1 IF $d(i)$ is $\tilde{A}_1$, THEN $v_{norm}(i) = c_1^A$
Rule 2 IF $d(i)$ is $\tilde{A}_2$, THEN $v_{norm}(i) = c_2^A$
$\vdots$
Rule L IF $d(i)$ is $\tilde{A}_L$, THEN $v_{norm}(i) = c_L^A$

and

Rule 1 IF $\Delta d(i)$ is $\tilde{B}_1$, THEN $\Delta v_{norm}(i) = c_1^B$
Rule 2 IF $\Delta d(i)$ is $\tilde{B}_2$, THEN $\Delta v_{norm}(i) = c_2^B$
$\vdots$
Rule L IF $\Delta d(i)$ is $\tilde{B}_L$, THEN $\Delta v_{norm}(i) = c_L^B$

where $\tilde{A}_j (j = 1,\ldots,L)$ and $\tilde{B}_j$ are the j-th antecedent fuzzy set for two fuzzy inputs $d(i)$ and $\Delta d(i)$; c_j^A and c_j^B are consequent constants at the j-th rule; L is the fuzzy rule number. The confidence of each antecedent at the j-th rule is obtained by

$$\omega_j^A = \mu_{Aj}\{d(i)\} \quad \ldots\ldots\ldots\ldots\ldots (15)$$

$$\omega_j^B = \mu_{Bj}\{\Delta d(i)\} \quad \ldots\ldots\ldots\ldots\ldots (16)$$

where $\mu_X(\bullet)$ denotes the confidence of a fuzzy set labeled by X. The fuzzy feed rate and its compensation are calculated by

$$v_{norm}(i) = \frac{\sum_{j=1}^{L} c_j^A \omega_j^A}{\sum_{k=1}^{L} \omega_k^A} \quad \ldots\ldots\ldots\ldots\ldots (17)$$

$$\Delta v_{norm}(i) = \frac{\sum_{j=1}^{L} c_j^B \omega_j^B}{\sum_{k=1}^{L} \omega_k^B}. \quad \ldots\ldots\ldots\ldots\ldots (18)$$

Resultant fuzzy feed rate $\tilde{v}_{norm}(i)$ is estimated from

$$\tilde{v}_{norm}(i) = v_{norm}(i) + \Delta v_{norm}(i). \quad \ldots\ldots\ldots\ldots\ldots (19)$$

$\tilde{v}_{norm}(i)$ is substituted into feed rate norm $\|\boldsymbol{v}_t(k)\|$ in Eq.(6), yielding

$$v_{tj}(k) = \tilde{v}_{norm}(i) \frac{t_j(i)}{\|\boldsymbol{t}(i)\|} \qquad (j = x,y,z). \quad \ldots\ldots (20)$$

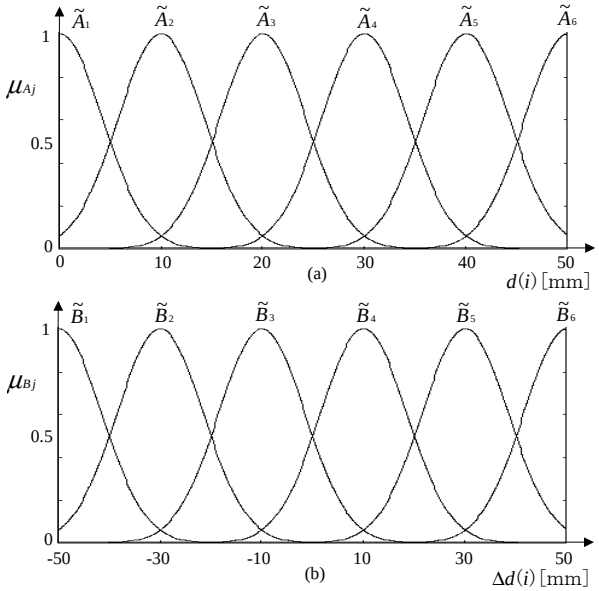

Fig. 4. Antecedent membership functions. Above is designed for $d(i)$ and below for $\Delta d(i)$.

Figure 4 shows antecedent membership functions designed for $d(i)$ and $\Delta d(i)$. The fuzzy set used is the following Gaussian membership function

$$\mu_X(x) = \exp\{\log(0.5)(x-\alpha)^2\beta^2\} \quad \ldots\ldots (21)$$

where α is the center of the membership function and β is the reciprocal of standard deviation. Reciprocals of the standard deviation are 0.2 and 0.1. Corresponding constants in the consequent part are listed in **Table 1**, in which $v_{\max}$ and $v_{\min}$ are the maximum and minimum values for the feed rate estimated in advance; v_{base} denotes $v_{\max} - v_{\min}$. These fuzzy rules are tuned based on the experience of a skilled operator. Note that the fuzzy reasoning part yields values larger than $v_{\max}$ and values smaller than $v_{\min}$ with the $d(i)$ and $\Delta d(i)$ combination.

4. Hybrid Position/Force Control with Weak Coupling

4.1. Handling of Polishing Force

In the polishing strategy dealing with polishing force [8, 9], polishing force is generated between an abrasive

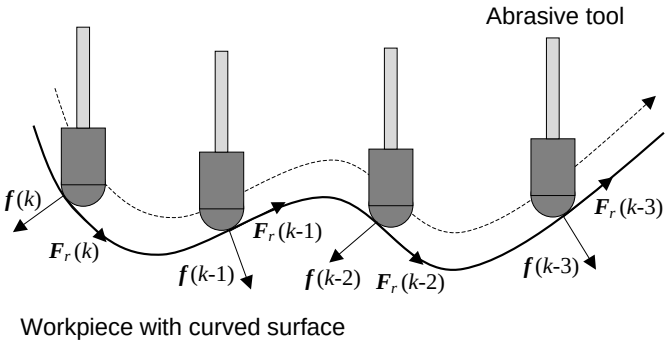

Fig. 5. Polishing force composed of contact force $\boldsymbol{f}$ and kinetic friction force $\boldsymbol{F}_r$.

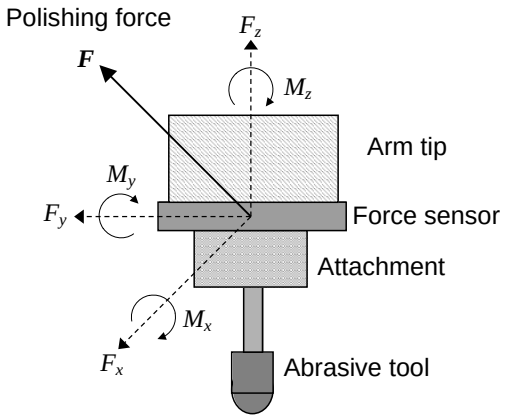

Fig. 6. 6-DOF force/torque sensor fixed between arm tip and abrasive tool attachment.

tool and a workpiece, and is the most important physical factor affecting polishing quality. Polishing force $\boldsymbol{F}(k) = [F_x(k)\ F_y(k)\ F_z(k)]^T$ is assumed to result from contact force $\boldsymbol{f}(k) = [f_x(k)\ f_y(k)\ f_z(k)]^T$ and kinetic friction force $\boldsymbol{F}_r(k) = [F_{rx}(k)\ F_{ry}(k)\ F_{rz}(k)]^T$ (**Fig.5**), so $\boldsymbol{F}(k)$ is written by

$$\boldsymbol{F}(k) = \boldsymbol{F}_r(k) + \boldsymbol{f}(k). \quad \ldots\ldots\ldots\ldots \quad (22)$$

To protect the mold surface against over-polishing, abrasive tool rotation is locked, and the workpiece is polished using kinetic friction force assumed to result from Coulomb friction force and viscous friction force. Each friction force is generated by contact force and tangential velocity, respectively. $\boldsymbol{F}(k)$ consisting of $\boldsymbol{F}_r(k)$ in tangential direction and $\boldsymbol{f}(k)$ in normal direction is measured by a 6 degree-of-freedom (DOF) force/torque sensor (**Fig.6**). Error $E(k)$ of polishing force magnitude is obtained by

$$E_f(k) = F_d - ||\boldsymbol{F}(k)|| \quad \ldots\ldots\ldots\ldots \quad (23)$$

where F_d is desired polishing force. Moment components M_x, M_y, and M_z are not used in our proposal.

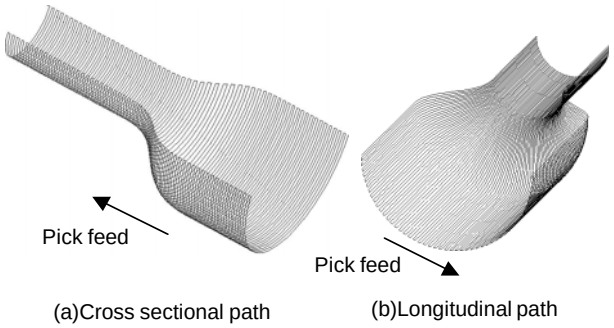

Fig. 7. CL data generated by a 3D CAD/CAM.

4.2. Feedback Control of Polishing Force

We present hybrid position/force control with weak coupling for polishing a curved workpiece. To avoid critical interference between the abrasive tool and the curved workpiece, the orientation of the abrasive tool is maintained fixed to the *z*-axis in base coordinates. If a workpiece has no overhang (**Fig.5**), a suitable contact point between the ball-end abrasive tool and the workpiece is maintained. Polishing is conducted by both the tangential velocity $\boldsymbol{v}_t(k)$ and normal velocity $\boldsymbol{v}_n(k)$ at the contact point (**Fig.5**).

We have proposed an impedance model following force control [1] for a 3D robot sander that flexibly sands woody workpieces with curved surfaces. In our proposed hybrid control, force control is applied only in the normal direction at the contact point, and the control law generates velocity scalar $v_{normal}(k)$ given by

$$v_{normal}(k) = v_{normal}(k-1)\ e^{-\frac{B_d}{M_d}\Delta t} + \left(e^{-\frac{B_d}{M_d}\Delta t} - 1\right)\frac{K_f}{B_d}E_f(k) \quad \ldots \quad (24)$$

where K_f is force feedback gain. M_d and B_d are the desired mass and desired damping coefficients. Δt is sampling width. Using $v_{normal}(k)$, normal velocity vector $\boldsymbol{v}_n(k)$ to control polishing force is represented by

$$\boldsymbol{v}_n(k) = v_{normal}(k)\frac{\boldsymbol{o}_d(k)}{||\boldsymbol{o}_d(k)||}. \quad \ldots\ldots\ldots \quad (25)$$

4.3. Feedforward and Feedback Controls of Tool Position

Molds used for PET bottle manufacturing are designed and machined with 3D CAD/CAM systems and machining centers. CL data $\tilde{\boldsymbol{P}}(i)$ generated by the main-processor of the CAM are used for the desired trajectory of the abrasive tool. The tool paths as shown in **Fig.7** are calculated in advance based on zigzag paths, and considered to be desired trajectories at the tip of the abrasive tool. Note that the cross-sectional and longitudinal paths have longitudinal and cross-sectional constant pick feed. **Fig.8** shows the block diagram of the hybrid position/force control system implemented in the polishing robot. The position of

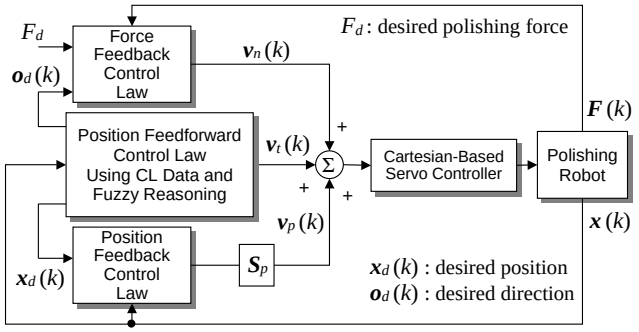

Fig. 8. Block diagram of hybrid position/force control.

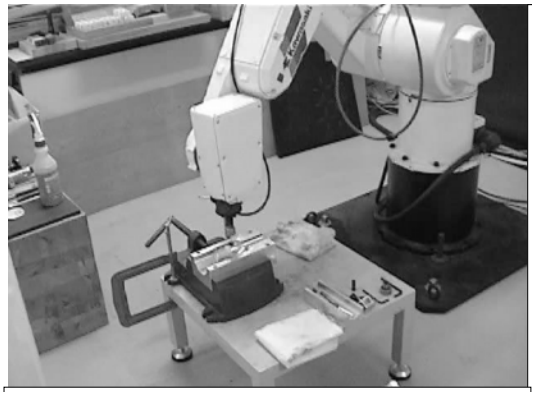

Fig. 9. Experimental setup based on industrial robot JS-10.

the abrasive tool is controlled feedforwardly by tangential velocity $\boldsymbol{v}_t(k)$ given by Eq.(20). $\boldsymbol{v}_t(k)$ is given through an open-loop action to avoid disturbing $\boldsymbol{v}_n(k)$. Polishing force is feedback-controlled by $\boldsymbol{v}_n(k)$, which is perpendicular to $\boldsymbol{v}_t(k)$. $\boldsymbol{v}_n(k)$ is given in the normal direction referencing $\boldsymbol{o}_d(k)$ as shown in Eq.(25). Note, however, that using only $\boldsymbol{v}_t(k)$ is not enough to execute desired trajectory control along CL data: the abrasive tool cannot move regularly, e.g., with a given pick feed of 0.2mm. To overcome this problem, a simple position feedback loop with small gains is added (**Fig.8**) so the abrasive tool does not deviate from the desired trajectory. The position feedback control law generates another velocity $\boldsymbol{v}_p(k)$ given by

$$\boldsymbol{v}_p(k) = \boldsymbol{S}_p \left\{ \boldsymbol{K}_p \boldsymbol{E}_p(k) + \boldsymbol{K}_i \sum_{n=1}^{k} \boldsymbol{E}_p(n) \right\} \quad \ldots \quad (26)$$

where $\boldsymbol{S}_p = \mathrm{diag}(S_{px}, S_{py}, S_{pz})$ is the switch matrix to construct coupling control in each direction. If $\boldsymbol{S}_p = \mathrm{diag}(1,1,1)$, then coupling control is active in all directions. If $\boldsymbol{S}_p = \mathrm{diag}(0,0,0)$, then the position feedback loop does not contribute to the force feedback loop in all directions. $\boldsymbol{E}_p(k) = \boldsymbol{x}_d(k) - \boldsymbol{x}(k)$ is position error, and $\boldsymbol{x}(k) = [x(k)\ y(k)\ z(k)]^T$ is the position vector at the tip of the abrasive tool obtained through forward kinematics. $\boldsymbol{K}_p = \mathrm{diag}(K_{px}, K_{py}, K_{pz})$ and $\boldsymbol{K}_i = \mathrm{diag}(K_{ix}, K_{iy}, K_{iz})$ are the position feedback gain and its integral gain matrices. Each component of $\boldsymbol{K}_p$ and $\boldsymbol{K}_i$ must be carefully set to small values to avoid disturbing the force control loop. Velocities $\boldsymbol{v}_n(k)$, $\boldsymbol{v}_t(k)$, and $\boldsymbol{v}_p(k)$ are summed and those are given to the reference of the Cartesian-based servo controller of the industrial robot. Six constraints, consisting of 3-DOF positions and 3-DOF forces in a constraint frame, cannot be satisfied simultaneously [10], but the delicate cooperation between the position and force feedback loops is an important key to successfully achieve robotic mold polishing.

5. Experiments

5.1. Experimental Setup

To evaluate the validity and effectiveness of the proposed polishing robot, we conducted a basic polishing experiment using an aluminum mold machined by an NC machine tool. The main objective of basic polishing is to remove all cusp marks on the surface whose heights are roughly 0.3mm. Basic polishing before finishing is one of the most important processes in maximizing mirror finishing beauty. **Fig.9** shows the industrial robot JS-10 with open control architecture used in the experiment. The industrial robot provides several useful Windows API functions such as velocity control and kinematics.

Table 2. Polishing conditions in using longitudinal path in **Fig.7**.

Longitudinal pick feed (mm)	0.2
Radius of abrasive tool R (mm)	5
Grain size of abrasive tool	#220, #320, #400
Rotational velocity of 6-th axis (°/s)	40 or -40
Rotational limits of 6-th axis	$-90° < \theta_6 < 90°$
Desired polishing force F_d (kgf)	2
Desired mass coefficient M_d (kgf·s^2/mm)	0.01
Desired damping coefficient B_d (kgf·s/mm)	30
Force feedback gain in normal direction K_f	1
Position feedback P-gain K_{px}, K_{py}, K_{pz}	0.01, 0, 0.01
Position feedback I-gain K_{ix}, K_{iy}, K_{iz}	0.0001, 0, 0.0001
Switch matrix $\boldsymbol{S}_p$ for coupling control	diag(1, 0, 1)
Sampling width Δt (ms)	10

5.2. Polishing Conditions

The aluminum mold is fixed with a jig along the *y*-axis in robot base coordinates. CL data used are generated with a zigzag path longitudinally (**Fig.7(b)**). Since rotation of the abrasive tool is locked and the polishing task is conducted with kinetic friction force, the desired polishing force is set to 2kgf. Locking of tool rotation does not cause undesirable high-frequency vibration noise, which is the most serious problem in allocating the force sensor between the tip of the robot arm and the abrasive tool. Other polishing conditions in using the path in **Fig.7(b)** are listed in **Table 2**.

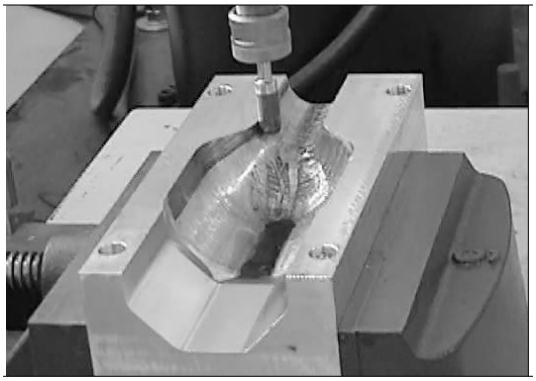

Fig. 10. Experimental scene using the polishing robot.

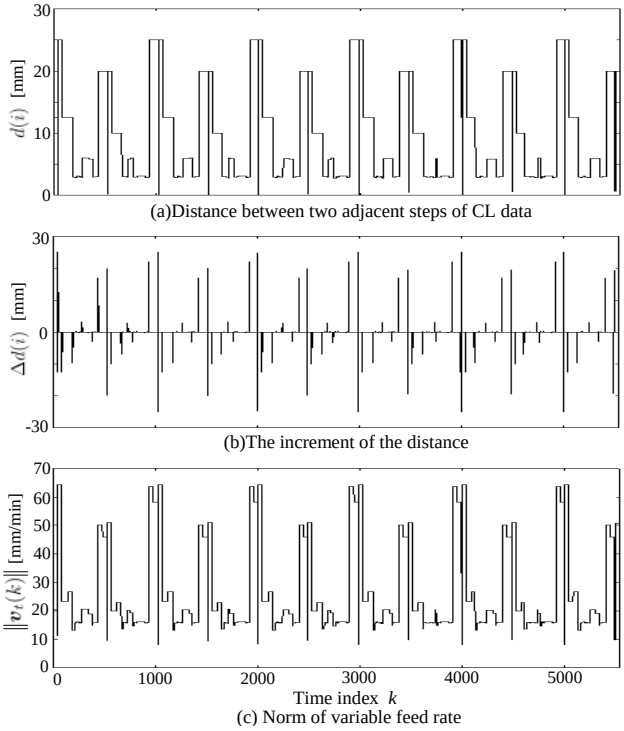

Fig. 11. Example of variable feed rate.

5.3. Polishing Task

Figure 10 shows polishing using the proposed robot. When the polishing robot runs, the abrasive tool rotates reciprocally at $\pm 40°$/s using the 6-th axis of the robot so the tool contour is abraded uniformly. If the abrasive tool is uniformly abraded maintaining the ball-end shape, the robot can keep up the initial performance of polishing. Although the tool length gradually became shorter due to abrasion, the force controller absorbed the uncertainty of the tool length. **Fig.11** shows results of the variable feed rate generated by the fuzzy reasoning, in which the zigzag path in **Fig.7(b)** is used. Above is $d(i)$, the middle is $\Delta d(i)$, and below is $||\boldsymbol{v}_t(k)||$ generated by the proposed fuzzy feed rate generator. $v_{\max}$ and $v_{\min}$ are 50mm/s and 10mm/s. We confirmed that the feed rate generator enabled the robot to reduce cycle time about 30% compared to without the generator. To obtain a higher quality surface, another zigzag path (**Fig.7(a)**) was used for the basic trajectory of the abrasive tool. The two passes shown in **Fig.7** were alternated.

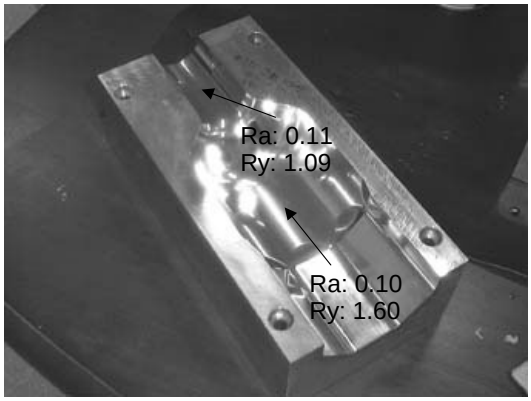

Fig. 12. Curved surface after wiping with a cloth containing polishing compound Cr_2O_3. $R_a(\mu m)$ and $R_y(\mu m)$ are arithmetical mean roughness and maximum depth.

The surface after polishing was evaluated visually and by touch, confirming a successful surface without overpolishing around the edges. Polishing force by the proposed hybrid position/force controller was more uniform on the average, than that of skilled workers, indicating the high degree of effective polishing. **Fig.12** shows the curved surface after wiping with a cloth containing polishing compound Cr_2O_3.

6. Conclusions

We have proposed an advanced feed rate generator using fuzzy reasoning for polishing robots to suitably regulate the feed rate along a free-formed surface. The feed rate generator determines the magnitude of variable velocity based on the curvature of each workpiece. We also designed a hybrid position/force controller for use with the feed rate generator. A mold polishing robot using the hybrid controller shortened cycle time during polishing of one workpiece dramatically to about 30% compared to the hybrid controller without the feed rate generator.

References:

[1] F. Nagata, K. Watanabe, and K. Izumi, "Furniture Polishing Robot Using a Trajectory Generator Based on Cutter Location Data," Procs. of IEEE International Conference on Robotics and Automation, pp. 319-324, 2001.

[2] F. Nagata, K. Watanabe, Y. Fujimoto et al., "3D Machining and Finishing System for New Designed Furniture," Procs. of the 2002 Japan-USA Symposium on Flexible Automation, pp. 1239-1245, 2002.

[3] F. Ozaki, M. Jinno, T. Yoshimi et al., "Force Controlled Finishing Robot System with a Task-Directed Robot Language," Journal of Robotics and Mechatronics, Vol.7, No.5, pp. 383-388, 1995.

[4] D. M. Gorinevsky, A. M. Formalsky, and A. YU. Schneider, "Force Control of Robotics Systems," CRC Press, 1997.

[5] F. Pfeiffer, H. Bremer, and J. Figueiredo, "Surface Polishing with Flexible Link Manipulators," European Journal of Mechanics, A/Solids, **15**, 1, pp. 137-153, 1996.

[6] Y. Takeuchi, D. Ge, and N. Asakawa, "Automated Polishing Process with a Human-like Dexterous Robot," Procs. of IEEE International Conference Robotics and Automation, pp. 950-956, 1993.
[7] P. R. Pagilla, and B. Yu, "Robotic Surface Finishing Processes: Modeling, Control, and Experiments," ASME Journal of Dynamic Systems, Measurement, and Control, **123**, pp. 93-102, 2001.
[8] F. Nagata, Y. Kusumoto, K. Watanabe et al., "Development of a Hybrid Motion/Force Control Strategy for Ball End Abrasive Tools and Its Application to Polishing Robots for PET Bottle Molds," Journal of the Japan Society for Precision Engineering, **70**, 1, pp. 59-64, 2004 (in Japanese).
[9] F. Nagata, K. Watanabe, Y. Kusumoto et al., "Generation of Normalized Tool Vector from 3-Axis CL Data and Its Application to a Mold Polishing Robot," Procs. of IEEE/RSJ International Conference on Intelligent Robots and Systems, pp. 3971-3976, 2004.
[10] J. J. Craig, "Introduction to ROBOTICS –Mechanics and Control Second Edition–," Addison Wesley Publishing Co., 1989.

Name:
Fusaomi Nagata

Affiliation:
Fukuoka Industrial Technology Center

Address:
3-6-1 Norimatsu, Yahatanishi, Kitakyushu, Fukuoka 807-0831, Japan

Brief Biographical History:
1985 Joined Kyushu Matsushita Electric Corp.
1989- Technical Researcher of Fukuoka Industrial Technology Center
2001- Special Researcher of Fukuoka Industrial Technology Center

Main Works:
- "Development of a Hybrid Motion/Force Control Strategy for Ball End Abrasive Tools and Its Application to Polishing Robots for PET Bottle Molds," Journal of the JSPE, 70-1, pp. 59-64, 2004.
- "Generation of Normalized Tool Vector from 3-Axis CL Data and Its Application to a Mold Polishing Robot," Procs. of 2004 IEEE/RSJ International Conference on Intelligent Robots and Systems (IROS2004), pp. 3971-3976, 2004.
- "An Open-Architecture-Based Hybrid Control Method with a Weak Coupling Between Position Feedback-Loop and Force Feedback-Loop," Transactions of the JSME, 71-701, pp. 178-184, 2005.

Membership in Learned Societies:
- The Japan Society for Precision Engineering (JSPE)
- The Japan Society of Mechanical Engineers (JSME)
- Robotics Society of Japan (RSJ)
- Japan Society for Fuzzy Theory and Intelligent Informatics (SOFT)

Name:
Keigo Watanabe

Affiliation:
Department of Advanced Systems Control Engineering, Graduate School of Science and Engineering, Saga University

Address:
1 Honjo-machi, Saga 840-8502, Japan

Brief Biographical History:
1980- Research Associate of Kyushu University
1985- Associate Professor of Shizuoka University
1990- Associate Professor of Saga University
1993- Professor of Saga University

Main Works:
- "An ART-Based Fuzzy Controller for the Adaptive Navigation of a Human-Coexistent Quadruped Robot," IEEE/ASME Trans. on Mechatronics, 7-3, pp. 318-328, 2002.
- "Modular Fuzzy-Neuro Controller Driven by Spoken Language Commands," IEEE Trans. on Systems, Man and Cybernetics, Part B, 34-1, pp. 293-302, 2004.
- "A Decentralized Control System for Cooperative Transformation by Multiple Nonholonomic Mobile Robots," Int. J. Control, 77-10, pp. 949-963, 2004.

Membership in Learned Societies:
- The Japan Society of Mechanical Engineers (JSME)
- The Japan Society for Precision Engineering (JSPE)
- The Japan Society for Aeronautical and Space Sciences
- The Society of Instrument and Control Engineers (SICE)
- The Institute of Systems, Control and Information Engineers (ISCIE)
- The Robotics Society of Japan (RSJ)
- Japan Society for Fuzzy Theory and Intelligent Informatics (SOFT)
- The Institute of Electrical and Electronics Engineers (IEEE)